05.2;06.1

Concentration of immobilized ε iron oxide nanoparticles as a basis for obtaining highly filled magnetically hard materials

© D.A. Balaev[1], V.L. Kirillov[2], A.A. Dubrovskiy[1], S.V. Semenov[1], Yu.V. Knyazev[1], M.N. Volochaev[1], O.N. Martyanov[2]

[1] Kirensky Institute of Physics, Federal Research Center KSC SB, Russian Academy of Sciences, Krasnoyarsk, Russia
[2] Boreskov Institute of Catalysis, Siberian Branch of RAS, Novosibirsk
E-mail: dabalaev@iph.krasn.ru

Received May 14, 2024
Revised July 17, 2024
Accepted July 17, 2024

The results of the study of the magnetic properties of the powder system of iron oxide nanoparticles ε-Fe_2O_3 (average size of 10 nm) are reported. The nanoparticles were obtained from a previously prepared composite material ε-Fe_2O_3/SiO_2 xerogel containing 20 wt.% ε-Fe_2O_3 by dissolving the SiO_2 matrix. The results of X-ray diffraction and Mossbauer spectroscopy confirmed the structure of ε-Fe_2O_3. From the analysis of magnetic measurements and the results of Mossbauer spectroscopy, it is possible to state the presence of a magnetic transition known for ε-Fe_2O_3 in the range of 75−150 K. This indicates the preservation of the magnetic characteristics of the particles after the matrix removal procedure and opens the possibility of obtaining a highly filled magnetically hard material based on epsilon-iron oxide.

Keywords: nanoparticles, ε-Fe_2O_3, Mossbauer spectroscopy, magnetization, magnetic transition.

DOI: 10.61011/TPL.2024.11.59671.19989

The current expansion of the application range of magnetic nanoparticles necessitates the development of efficient approaches to reproducible fabrication of nanomaterials [1–3] with specific magnetic characteristics. Nanoscale particles acquire new magnetic properties, which are not found in their bulk counterparts, due to the influence of surface and size effects [4–6]. However, the influence of a developed surface of nanoparticles may also manifest itself in the potential formation of structural polymorphs that exist only in nanoscale particles. A striking example of this is iron oxide ε-Fe_2O_3, which has been characterized reliably for the first time in [7]. It is produced in the form of particles no larger than 20−30 nm [6–12] or nanowires with linear dimensions up to ~ 100 nm [12,13].

ε-Fe_2O_3 nanoparticles have a record-strong coercive field Hc for oxide materials (~ 20 kOe for particles as small as $d \sim 20-30$ nm) [12,14]), which is important for practical applications. Since the ε-Fe_2O_3 structure requires the use of silicon oxide SiO_2 as a carrier matrix to form, most of the materials obtained are deposited and/or composite systems ε-Fe_2O_3/SiO_2, where magnetic nanoparticles are immobilized on the carrier surface or encapsulated in a SiO_2 matrix. It is difficult to obtain a system with a high ε-Fe_2O_3 concentration in this case, since particle agglomeration leads to the formation of other polymorphs of iron oxide [8–10]. At the same time, highly concentrated systems are needed for practical applications, since the relatively low saturation magnetization of ε-Fe_2O_3 (~ 15 emu/g) becomes significantly lower in a composite. One way to overcome this problem is to extract ε-Fe_2O_3 nanoparticles from the SiO_2 matrix while making sure that the magnetic properties of these particles remain unchanged. The choice of the method for extracting nanoparticles is determined by the carrier state, and the results of successful experiments on synthesis of pure powder of ε-Fe_2O_3 nanoparticles were reported in [14]. In the present study, we discuss one approach to the production of phase-pure ε-Fe_2O_3 nanoparticles that are extracted from the porous ε-Fe_2O_3/SiO_2 xerogel composite and free from the matrix material.

A sample of ε-Fe_2O_3 nanoparticles in a SiO_2 xerogel matrix, which contained 20 wt.% ε-Fe_2O_3, was synthesized in accordance with the procedure detailed in [15]. This sample is hereinafter referred to as the initial one. To extract ε-Fe_2O_3 nanoparticles from the matrix, the initial sample was dissolved in a 25% aqueous solution of tetramethylammonium hydroxide (TMAH) at 82°C within 14 h (TMAH/SiO_2 = 4). The resulting solution was filtered through a „blue ribbon“ paper filter (2.5 μm). ε-Fe_2O_3 nanoparticles were extracted from the transparent dark red filtrate by repeated magnetic decantation (over the course of 24 h) with an NdFeB magnet and rinsed with ethanol to a neutral pH value. More than 90% of ε-Fe_2O_3 (relative to the initial iron oxide content) were extracted in 18 consecutive magnetic decantation cycles. The resulting sample is referred to as the extracted one.

X-ray diffraction patterns were obtained using an XTRA powder diffractometer and CuK_α radiation. A Hitachi HT7700 transmission electron microscope (TEM) and a PPMS-9 setup were used for imaging and magnetic measurements (temperature and field dependences of magne-

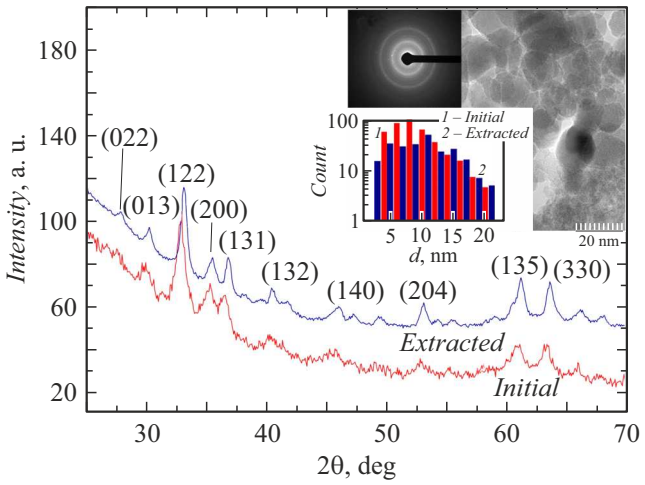

Figure 1. X-ray diffraction patterns of the initial and extracted samples. A typical TEM image, a microdiffraction pattern for a selected area of the extracted sample, and histograms of the particle size distribution for the examined samples in a semi-logarithmic scale are shown in the inset.

tization $M(T)$ and $M(H)$ and temperature dependences of the real part of magnetic susceptibility $\chi'(T)$), respectively. Mössbauer spectra were measured with an MS-1104Em spectrometer (Research Institute of Physics, Southern Federal University).

The peaks in the diffraction pattern of the extracted sample (Fig. 1) correspond to the ε-Fe_2O_3 phase. Figure 1 presents the typical results of microdiffraction and TEM studies and histograms of the particle size distribution for the initial and extracted samples. It may be concluded that the distributions are close in the region of particle sizes exceeding 10 nm, but the initial sample has a significantly higher fraction of particles smaller than 10 nm in diameter. Average particle size $\langle d \rangle$ of the extracted sample is ~ 10.5 nm (the corresponding value for the initial sample is slightly smaller, since the fraction of small particles is higher: $\langle d \rangle \approx 8.5$ nm).

Figure 2, *a* shows the ^{57}Fe Mössbauer spectra of the initial and extracted samples at two different temperatures ($T = 4.2$ and 300 K). The hyperfine parameters of spectra are in complete agreement with those determined earlier for ε-Fe_2O_3 particles [16,17]. The results of processing of spectra reveal four characteristic nonequivalent iron sites in the ε-Fe_2O_3 structure, which are denoted as Fe(1+2), Fe3, and Fe4. The last site differs from the first three in having a tetrahedral oxygen environment. The parameters of samples at 4.2 K are identical. The quadrupole doublet observed in the center at 300 K corresponds to the fraction of particles that, according to the ^{57} Mössbauer spectroscopy data, are in the superparamagnetic state (SPM in Fig. 2, *a*). This fraction varies from 36% for the initial sample to 30% for the extracted one. This agrees with the TEM data and is probably attributable to „washing-off" of the smallest particles of the ε-Fe_2O_3 phase in the process of xerogel matrix removal.

Figure 2, *b* shows the magnetic hysteresis loops of the extracted and initial samples. At 300 K, coercive field H_C of the extracted sample is ~ 2.1 kOe (see the inset in Fig. 2, *b*). This is lower than the value of $H_C \sim 20$ kOe for „large" particles ($d \sim 20-30$ nm), since the average size in the present case is 2 times smaller; the classical effect of H_C reduction for single-domain particles with a reduction in their size due to the influence of thermal fluctuations [8,14] is manifested here. In addition, the distinct shape of hysteresis loops, which reach the maximum field width of hysteresis (ΔH at $M = \text{const}$) not in the vicinity of „zero magnetization", but at intermediate magnetization values, is indicative of a significantly wide coercive field distribution, where H_C reaches values greater than 10 kOe (see the horizontal segments in Fig. 2, *b*). The $M(H)$ dependences for the initial sample are also shown in Fig. 2, *b* for comparison. It is characterized by $H_C \approx 3.7$ kOe, which is somewhat higher than the value for the extracted sample. What is important here is that the specific magnetization of the extracted sample in sufficiently strong fields is almost 5 times (in inverse proportion to the concentration of ε-Fe_2O_3 in the initial sample) higher than the initial one.

The $H_C(T)$ dependence for the extracted sample is shown in Fig. 3, *a*. The nonmonotonic behavior of $H_C(T)$ reflects the presence of a known magnetic transition in ε-Fe_2O_3, which is somewhat of a „trademark" of the ε-Fe_2O_3 oxide [6,8,12,16–19]. A ferrimagnetic collinear structure is established in ε-Fe_2O_3 within the 150−500 K temperature range. The magnetic transition proceeds with a change in temperature in at least two stages with characteristic ranges of 150−110 and 110−75 K [18] (denoted by vertical dashed lines in Fig. 3). In the vicinity of 75 K, the value of H_C is minimal and it may be assumed that ε-Fe_2O_3 has a non-collinear magnetic structure of the magnetic spiral type [17]. This $H_C(T)$ behavior correlates with the temperature dependence of hyperfine field H_{hf} for iron in a tetrahedral oxygen environment (Fe4) (Fig. 3, *a*), which was determined by analyzing the Mössbauer spectra. The hyperfine field at the Fe4 site is the most sensitive to this magnetic transition and undergoes a sharp increase within the 150−75 K temperature range [16].

The shape of the $M(T)$ and $\chi'(T)$ dependences (Fig. 3, *b*) of the extracted sample is also indicative of the presence of a magnetic transition. The $M(T)$ dependences were measured in the zero field cooling (ZFC), field-cooled cooling (FCC), and field-cooled warming (FCW) regimes. The behavior of the $M(T)$ dependences changes at characteristic temperatures of 150, 110, and 75 K (marked with vertical dashed lines). The thermomagnetic history starts to have an effect at a temperature slightly below 150 K, when the magnetic structure begins to change. Temperature hysteresis for the FCC and FCW regimes in the second interval (110−75 K) of the magnetic transition is worthy of note. A characteristic

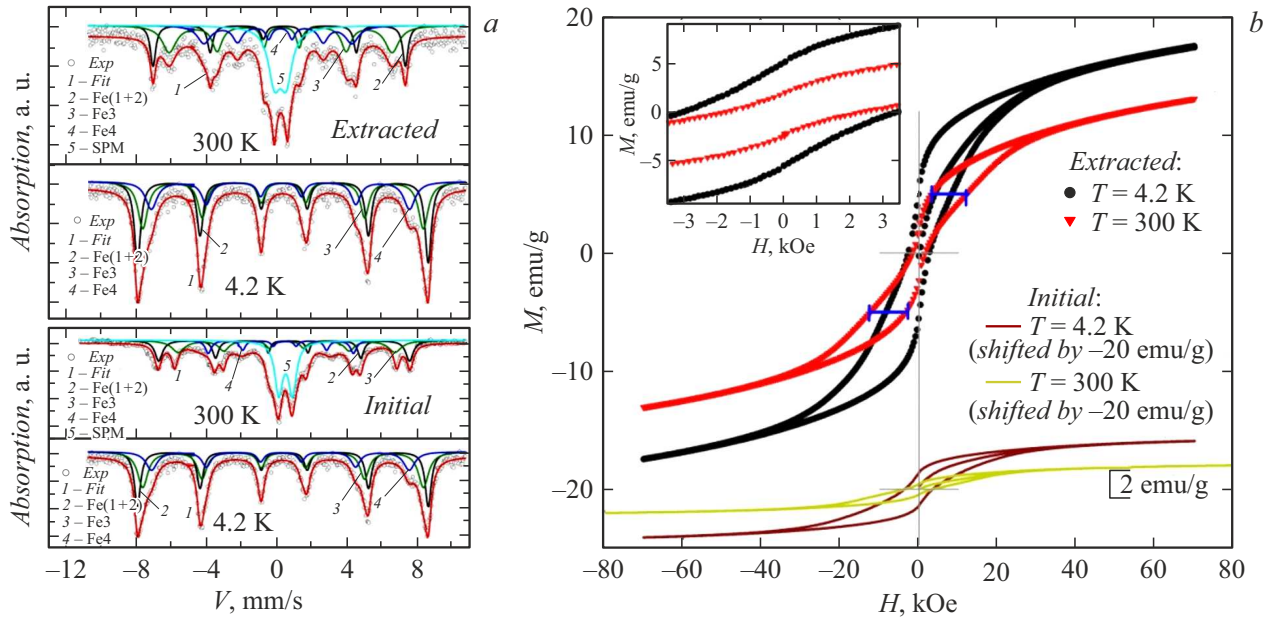

Figure 2. *a* — Mössbauer spectra (dots) of the initial and extracted samples at $T = 4.2$ and 300 K with processing results (solid curves). *b* — Magnetization hysteresis loops $M(H)$ of the initial and extracted samples at $T = 4.2$ and 300 K normalized to the material (sample) mass. The magnetization data for the initial sample are shifted along the ordinate axis by -20 emu/g. The inset presents the $M(H)$ dependences for the extracted sample in the vicinity of the origin of coordinates.

maximum of magnetic susceptibility $\chi'(T)$ is found within the same temperature interval (the $\chi'(T)$ dependences were measured for samples without magnetic history in zero external field with an alternating field amplitude of 2 Oe). The maximum shifts to the region of lower temperatures with increasing frequency of the alternating field, which is a distinct, but still unexplained feature of the magnetic transition in ε-Fe_2O_3 [19]. A collinear ferrimagnetic structure is established above 150 K, and the magnetic susceptibility becomes independent of frequency.

The $\chi'(T)$ dependences for the initial sample are shown in Fig. 3, *b* for comparison. These dependences feature two maxima. It was noted in [6] that superparamagnetic (SPM) blocking is observed at temperatures below ~ 70 K for ε-Fe_2O_3 particles smaller than ~ 6 nm. Therefore, the low-temperature susceptibility maximum for the initial sample is associated with SPM blocking of small (smaller than 6 nm) particles. An additional confirmation of the above is the shift of the $\chi'(T)$ dependence maximum toward higher temperatures with increasing frequency, which is characteristic of SPM blocking processes. The lack of a low-temperature maximum in the $\chi'(T)$ dependences for the extracted sample suggests that it features a lower fraction of small ($d < 6$ nm) particles than the initial sample. This correlates well with the results obtained above.

Thus, the magnetic characteristics of ε-Fe_2O_3 particles extracted from the matrix remained the same as the ones measured in the initial sample with ε-Fe_2O_3 particles in the SiO_2 xerogel matrix, but the fraction of particles smaller than ~ 6 nm in diameter became lower. The specific magnetization of the obtained sample of ε-Fe_2O_3 nanoparticles is several times higher than the magnetization of composite samples containing ε-Fe_2O_3. ε-Fe_2O_3 nanoparticles synthesized in powder form may serve as a basis for a highly filled magnetically hard material that is promising for practical applications.

Acknowledgments

Equipment provided by the common use center of the Federal Research Center „Krasnoyarsk Science Center of the Siberian Branch of the Russian Academy of Sciences“ was used for $\chi'(T)$ measurements and TEM studies.

The authors wish to thank O.A. Bayukov and A.A Krasikov for fruitful discussions.

Funding

This research was supported by grant No. 24-12-20011 (https://rscf.ru/project/24-12-20011/) from the Russian Science Foundation and the Krasnoyarsk Regional Science Foundation.

Conflict of interest

The authors declare that they have no conflict of interest.

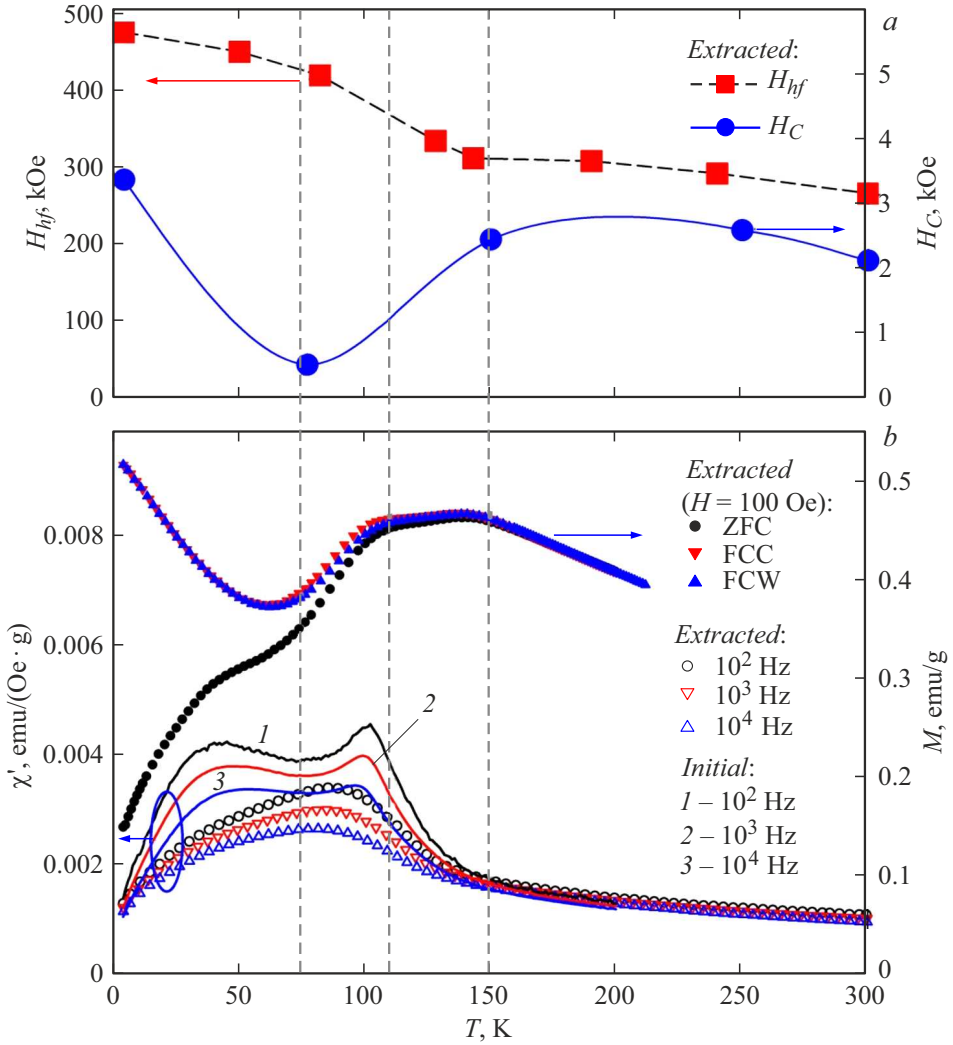

Figure 3. *a* — Temperature evolution of hyperfine field H_{hf} for the Fe4 site and coercive field H_C of the extracted sample. *b* — Temperature dependences of magnetic susceptibility $\chi'(T)$ at different frequencies for the initial and extracted samples and magnetization $M(T)$ for the extracted sample with different thermomagnetic histories. The susceptibility and magnetization data are normalized to the mass of ε-Fe_2O_3.

References

[1] A.S. Kamzin, A. Bingolbali, N. Doğan, Z. Yeşil, M. Asilturk, Tech. Phys. Lett., **45** (10), 1008 (2019). DOI: 10.1134/S1063785019100092.

[2] A Omelyanchik, K. Levada, S. Pshenichnikov, M. Abdolrahim, M. Baricic, A. Kapitunova, A. Galieva, S. Sukhikh, L. Astakhova, S. Antipov, B. Fabiano, D. Peddis, V. Rodionova, Materials, **13**, 5014 (2020). DOI: 10.3390/ma13215014

[3] A.S. Kamzin, V.G. Semenov, L.S. Kamzina, Phys. Solid State, **66** (4), 603 (2024). DOI: 10.61011/PSS.2024.04.58207.44.

[4] A. Omelyanchik, A.S. Kamzin, A.A. Valiullin, V.G. Semenov, S.N. Vereshchagin, M. Volochaev, A. Dubrovskiy, T. Sviridova, I. Kozenkov, E. Dolan, D. Peddis, A. Sokolov, V. Rodionova, Coll. Surf. A, **647**, 129090 (2022). DOI: 10.1016/j.colsurfa.2022.129090

[5] Yu.V. Knyazev, D.A. Balaev, V.L. Kirillov, O.A. Bayukov, O.N. Mart'yanov, JETP Lett., **108** (8), 527 (2018). DOI: 10.1134/S0021364018200092.

[6] D.A. Balaev, A.A. Dubrovskiy, Yu.V. Knyazev, S.V. Semenov, V.L. Kirillov, O.N. Martyanov, Phys. Solid State, **65** (6), 938 (2023). DOI: 10.21883/PSS.2023.06.56105.12H.

[7] E. Tronc, N. Chaneac, J.P. Jolivet, J. Solid State Chem., **139**, 93 (1998). DOI: 10.1006/jssc.1998.7817

[8] D.A. Balaev, S.S. Yakushkin, A.A. Dubrovskii, G.A. Bukhtiyarova, K.A. Shaikhutdinov, O.N. Martyanov, Tech. Phys. Lett., **42** (4), 347 (2016). DOI: 10.1134/S1063785016040039.

[9] D.O. Testov, K.G. Gareev, I.K. Khmelnitskiy, A. Kosterov, L. Surovitskii, V.V. Luchinin, Magnetochemistry, **9**, 10 (2023). DOI: 10.3390/magnetochemistry9010010

[10] E. Gorbachev, M. Soshnikov, M. Wu, L. Alyabyeva, D. Myakishev, E. Kozlyakova, V. Lebedev, E. Anokhin, B. Gorshunov, O. Brylev, P. Kazin, L. Trusov, J. Mater. Chem. C, **9**, 6173 (2021). DOI: 10.1039/d1tc01242h

[11] I. Edelman, J. Kliava, O. Ivanova, R. Ivantsov, D. Velikanov, V. Zaikovskii, E. Petrakovskaja, Y. Zubavichus, S. Stepanov, J. Non-Cryst. Solids, **506**, 68 (2019). DOI: 10.1016/j.jnoncrysol.2018.12.006
[12] J. Tucek, R. Zboril, A. Namai, S. Ohkoshi, Chem. Mater., **22**, 6483 (2010). DOI: 10.1021/cm101967h
[13] A.I. Dmitriev, Tech. Phys. Lett., **44** (2), 137 (2018). DOI: 10.1134/S1063785018020207.
[14] S. Ohkoshi, A. Namai, K. Imoto, M. Yoshikiyo, W. Torora, K. Nakagawa, M. Komine, Y. Miyamoto, T. Nasu, S. Oka, H. Tokoro, Sci. Rep., **5**, 14414 (2015). DOI: 10.1038/srep14414
[15] S.S. Yakushkin, D.A. Balaev, A.A. Dubrovskiy, S.V. Semenov, Yu.V. Knyazev, O.A. Bayukov, V.L. Kirillov, R.D. Ivantsov, I.S. Edelman, O.N. Martyanov, Ceram. Int., **44**, 17852 (2018). DOI: 10.1016/j.ceramint.2018.06.254
[16] Yu.V. Knyazev, A.I. Chumakov, A.A. Dubrovskiy, S.V. Semenov, S.S. Yakushkin, V.L. Kirillov, O.N. Martyanov, D.A. Balaev, JETP Lett., **110** (9), 613 (2019). DOI: 10.1134/S0021364019210082.
[17] Yu.V. Knyazev, A.I. Chumakov, A.A. Dubrovskiy, S.V. Semenov, I. Sergueev, S.S. Yakushkin, V.L. Kirillov, O.N. Martyanov, D.A. Balaev, Phys. Rev. B, **101**, 094408 (2020). DOI: 10.1103/PhysRevB.101.094408
[18] C.R.S. Haines, M. Gich, J.L. García-Muñoz, A. Romaguera, Z. Ma, M.B. Costa, M.A. Carpenter, J. Magn. Magn. Mater., **583**, 170240 (2023). DOI: 10.1016/j.jmmm.2022.170240
[19] R. Jones, R. Nickel, P.K. Manna, J. Hilman, J. van Lierop, Phys. Rev. B, **100**, 094425 (2019). DOI: 10.1103/PhysRevB.100.094425

Translated by D.Safin